

Sulfur Conversion to Multifunctional Poly(*O*-thiocarbamate)s through Multicomponent Polymerizations of Sulfur, Diols, and Diisocyanides

Jie Zhang, Qiguang Zang, Fulin Yang, Haoke Zhang, Jing Zhi Sun,* and Ben Zhong Tang*

Cite This: *J. Am. Chem. Soc.* 2021, 143, 3944–3950

Read Online

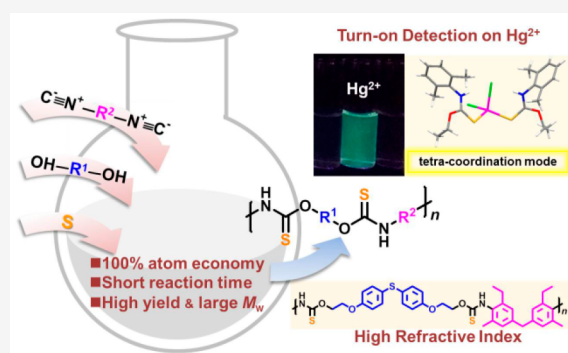
ACCESS |

Metrics & More

Article Recommendations

Supporting Information

ABSTRACT: Sulfur, which is generated from the waste byproducts in the oil and gas refinery industry, is an abundant, cheap, stable, and readily available source in the world. However, the utilization of excessive amounts of sulfur is mostly limited, and developing novel methods for sulfur conversion is still a global concern. Here, we report a facile one-step conversion from elemental sulfur to functional poly(*O*-thiocarbamate)s through a multicomponent polymerization of sulfur, diols, and diisocyanides, which possesses a series of advantages such as mild condition (55 °C), short reaction time (1 h), 100% atom economy, and transition-metal free in the catalyst system. Seven poly(*O*-thiocarbamate)s are constructed with high yields (up to 95%), large molecular weight (up to 53100 of M_w), good solubility in organic solvents, and completely new polymer structures. The poly(*O*-thiocarbamate)s possess a high refractive index above 1.7 from 600 to 1700 nm by adjusting the sulfur content. By incorporating tetraphenylethene (TPE) moieties into the polymer structure, the poly(*O*-thiocarbamate)s can also be designed as fluorescent sensors to detect harmful metal cation of Hg^{2+} in a turn-on mode with high sensitivity (LOD = 32 nM) and excellent selectivity (over interference cations of Pb^{2+} , Au^{3+} , Ag^+). Different from the previous reports, the exact coordination structure is first identified by single-crystal X-ray diffraction, which is revealed in a tetracoordination fashion (two sulfur and two chloride) using a model coordination compound.



INTRODUCTION

The utilization of sulfur can be dated back to ancient times, as documented in Ancient Greek, Roman, and Chinese history. Although studied for centuries, sulfur-related studies remain hot spots in the areas of chemistry, biology, and geology.^{1–12} With the yearly increase of the oil and gas refinery industry, it is reported that more than 80 million metric tons of sulfur are globally produced.^{13,14} The excessive amounts of sulfur may find their way out in polymer chemistry.¹⁵ As a simple, cheap, and readily available starting material, sulfur is well suited as a monomer in polymerization. Meanwhile, compared with traditionally smelly or unstable sulfur-containing reagents such as thiols, episulfide, isothiocyanates, and carbon disulfide,¹⁶ elemental sulfur is an abundant source for sulfur-containing polymers due to its odorlessness and stability. Sulfur-containing polymers have drawn increasing attention for their various optoelectronic applications and unique metal-coordination capacity.^{17–19} However, the methods for preparing sulfur-containing polymers using elemental sulfur are extremely limited.²⁰ Only a handful of research has been reported including vulcanization, inverse vulcanization,^{15,21} multicomponent polymerizations (MCPs) of elemental sulfur,^{22–26} and copolymerization of episulfide and elemental sulfur.^{27,28}

Among these methods, MCPs have stood out on sulfur conversion. For example, polythioamides constructed by sulfur, amines, and aldehydes were synthesized through a typical MCP route.^{22,23} In the past five years, Tang et al. have reported the MCPs of sulfur, amines and diynes,²⁴ the MCPs of sulfur, diamines, and isocyanides²⁵ and the MCPs of sulfur, aliphatic diamines, and acids²⁶ in succession. MCPs are becoming a powerful tool for sulfur conversion to functional polymers. However, amines are invariably relied on among all of the above-mentioned MCPs. As a result, the generalization of sulfur conversion to polymers will be extremely limited. Compared with amides, alcohols are cheaper, more eco-friendly, storage-stable, and achievable. Similar to amines, alcohols also possess nucleophilicity,^{29–31} which is proved by its reaction with sulfur and isocyanides.³² So, alcohols are expected reasonably to break the limitation on monomers and to be considered as ideal raw materials.

Received: January 8, 2021

Published: March 4, 2021



Herein, MCPs of sulfur, alcohols, and isocyanides are explored. The incorporation of elemental sulfur by MCPs permitted the placement of sulfur atoms in polymer main chains easily and efficiently, producing a series of poly(*O*-thiocarbamate)s with high molecular weight (M_w) thiocarbamate during a short period in high yields. It is noteworthy that only base was used in the polymerization as catalyst but without any transition-metal catalysts. Furthermore, to the best of our knowledge, poly(*O*-thiocarbamate)s were unprecedentedly prepared; thus, they could become a new family of functional polymers. In addition, thanks to the involvement of sulfur, poly(*O*-thiocarbamate)s possess high refractive index, showing potential as advanced optical materials. More importantly, elemental sulfur efficiently converted to thione, and taking advantage of the unique coordination between thione and mercury cation (Hg^{2+}), poly(*O*-thiocarbamate)s were designed to be fluorescent chemosensors for Hg^{2+} in a turn-on mode with high sensitivity and good selectivity. Different from the previous reports,^{25,33–46} the coordination structure was first revealed using single-crystal X-ray diffraction for model coordination compound, which clarifies the detection mechanism.

RESULTS AND DISCUSSION

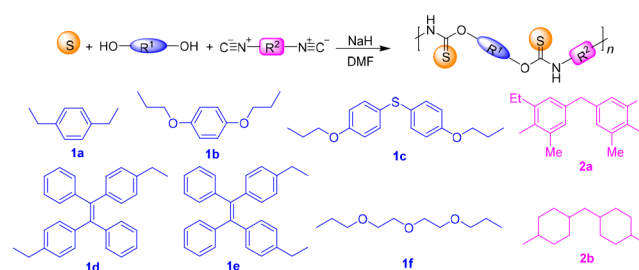
MCPs of Sulfur, Diols and Diisocyanides. First, the reaction mechanism was investigated using a model reaction of sulfur, diol 3, and isocyanide 4 (Scheme S1). Sulfur and NaH were initially mixed in solvent, generating sodium polysulfide. Five minutes later, isocyanide was added and then attacked by sodium polysulfide. Isothiocyanate 5 was separated as the sole key intermediate (Figure S1-A). It is noteworthy that the feeding sequence is of crucial importance for the formation of 5. If sulfur/NaH/isocyanide were fed together, there were impurities as shown in Figure S1-B. Afterward, ethanol was added, producing the end product M1 with the promotion of NaH. After understanding the reaction mechanism of the three components, we set about developing the MCPs of sulfur, diols, and diisocyanides.

Polymerization conditions are key parameters, which have direct effects on the derived polymers. To systematically optimize various conditions, economic sublimed sulfur, cheap alcohol 1a, and easily prepared diisocyanide 2a were chosen as an example. The polymerization was first carried out by a stoichiometric ratio of monomers at 40 °C in THF, producing a low M_w polymer in 53% yield (entry 1, Table S1). The excess amount of sulfur and NaH could significantly improve the yield and M_w of the product. When the ratio of $[S]/[NaH]/[1a]$ reached 4:4:1, the M_w of polymer was as high as 10000 (entry 3, Table S1). Increasing or decreasing monomer concentration could not promote the polymerization, so 0.2 M was chosen as the optimal concentration. The temperature had a big influence on the MCPs. At room temperature, both the yield and the M_w of the product were undesired. After the temperature was raised to 55 °C, the yield was dramatically increased to above 90%, probably due to the enhanced solubility of sodium polysulfide in THF. A better result could not be obtained if the temperate continued to rise (entries 6–8, Table S1). Thus, the polymerization was carried out at 55 °C in subsequent explorations. Time-optimizing experiments indicated that 1 h was enough for the completion of the MCP (entry 10, Table S1). The short period of polymerization was strong motivator for the popularization of the MCP. Apart from THF, the solvent was changed into three other polar

solvents (*N,N'*-dimethyl formamide, dimethyl sulfoxide, and *N*-methylpyrrolidone). Surprisingly, the best result was obtained in *N,N'*-dimethyl formamide (DMF), and polymer with a M_w of 24600 was furnished in 90% yield (entry 13, Table S1).

To explore monomer scope and endow products with functions, a series of diols 1a–f and aromatic/aliphatic diisocyanides 2a,b were selected as monomers (Scheme 1).

Scheme 1. Polymerization of Sulfur, Diols, and Diisocyanides



The MCPs of all seven combinations of sulfur, six diols, and two diisocyanides were carried out in DMF at 55 °C for 1 h under nitrogen atmosphere. All of the polymerizations proceeded smoothly and rapidly to produce poly(*O*-thiocarbamate)s. The yields of the polymers were in the range of 81–95%, and the M_w was high, up to 53100 (Table 1,

Table 1. Polymerization of Sulfur, Diols, and Diisocyanides^a

polymer	monomers	yield (%)	M_w^b	M_n^b	\bar{D}	$M_n'^c$
P1	S + 1a + 2a	90	24600	14200	1.73	13134
P2	S + 1b + 2a	91	27600	16700	1.65	6401
P3	S + 1c + 2a	90	26400	16800	1.57	7224
P4	S + 1d + 2a	87	23900	13300	1.80	7663
P5	S + 1e + 2a	85	20800	13200	1.57	9179
P6	S + 1f + 2a	95	53100	26500	2.00	17394
P7	S + 1a + 2b	81	13400	8600	1.56	7509

^aCarried out in 1 mL of DMF at 55 °C under nitrogen atmosphere ($[1] = 0.2$ mmol/L, $[S] = 0.8$ mmol/L, $[1]/[2] = 1:1$, $[S]/[NaH] = 1:1$). ^b M_w and \bar{D} (M_w/M_n) of polymers were estimated by GPC in DMF on the basis of a polystyrene calibration. ^c M_n' of polymers were calculated by the method of integral area in ¹H NMR (Figure S5).

Figure S2). These features demonstrate the general monomer applicability and high efficiency. All polymers possess excellent solubility in common solvents and good thermal stability (Figure S3).

Characterization of the Poly(*O*-thiocarbamate)s. To facilitate the structural characterization, model compound M1 was prepared under the same reaction conditions (Scheme S2) and its structural accuracy was proved by the single-crystal structure (Table S2). Then the ¹H/¹³C NMR spectra of monomers 2a and 1a, model compound M1, and P1 in DMSO-*d*₆ were compared as shown in Figure 1. The resonance of –OH at δ 5.13 ppm disappeared in the ¹H NMR spectra of M1 and P1, while the resonance of C≡N at δ 167.95 entirely disappeared in the ¹³C NMR spectra of M1 and P1. The comparison indicated that monomers 1a and 2a have been consumed and polymerized. More importantly, a new broad peak “a” at δ 10.43 assigned to –NH– emerged in the

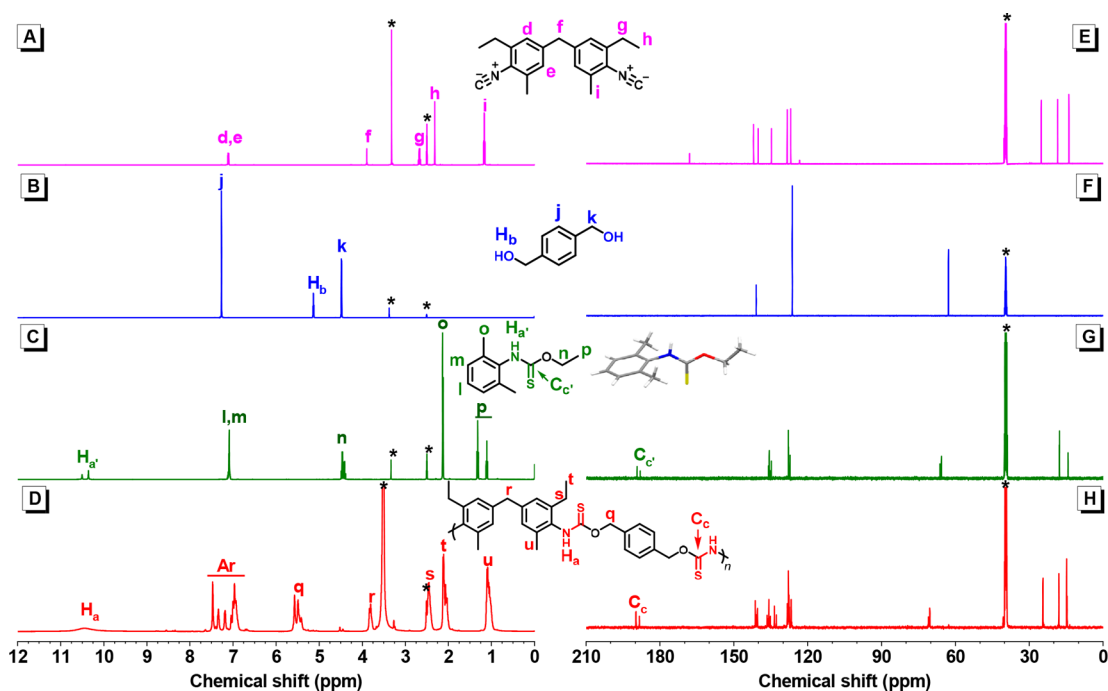


Figure 1. ^1H NMR spectra of monomers **2a** (A), **1a** (B), model compound **M1** (C), and polymer **P1** (D) in $\text{DMSO-}d_6$; ^{13}C NMR spectra of monomers **2a** (E), **1a** (F), model compound **M1** (G) and polymer **P1** (H) in $\text{DMSO-}d_6$.

^1H NMR spectrum of **P1**, which corresponded to the set of peaks “a” at δ 10.50–10.36 in the ^1H NMR spectrum of **M1**. Meanwhile, a set of peaks at δ 189.77–188.39 assigned to the thiocarbonyl “c” of **P1** was well-matched with “c” of **M1** at δ 189.28–188.04 in ^{13}C NMR (Figure 1G). As there was a conformational equilibrium between *cis*- and *trans*-orientations in the *O*-thiocarbamate group, a pronounced conformational split of the signal was observed in the NMR spectra of **M1** and **P1**, which had previously been found in analogous structures such as urea, thiourea, amide, and thioamide.^{47–49} All of these results manifested that the *O*-thiocarbamate linkage had been formed indeed. In addition, the structural characterization by FTIR also showed the vanishing of $\text{C}\equiv\text{N}/\text{OH}$ and the formation of $\text{C}=\text{S}/\text{NH}$ (Figure S4), reaching the same conclusion.

For other poly(*O*-thiocarbamate)s **P2**–**P7**, the characteristic NH peaks at δ 9.55–7.05 all emerged in their ^1H NMR spectra (Figure S5), and the characteristic $\text{C}=\text{S}$ peaks at δ 179.6–183.6 all emerged in their ^{13}C NMR spectra (Figure S6), besides the vibration of $\text{C}=\text{S}$ at $1505\text{--}1490\text{ cm}^{-1}$, and the vibration NH at $3354\text{--}3218\text{ cm}^{-1}$ all emerged in their FTIR spectra (Figure S7–12), confirming the expected poly(*O*-thiocarbamate) structure.

High Refractive Index. High refractive index (n) materials play an irreplaceable role in the achievement of large-scale photonic integration due to their compact structure.^{50,51} However, the vast majority of organic polymers exhibit relatively low n -values of 1.5–1.6.^{52,53} In contrast, high refractive index polymers (HRIPs, where $n \geq 1.7$) have drawn increasing attention for their various optoelectronic applications such as organic light-emitting diodes, microlens components in both charge-coupled devices, high-performance complementary image sensors,^{54,55} all-polymer optoelectronic devices,⁵⁶ and polymer-based optical waveguides.⁵⁰ It is well-known that introduction of sulfur atoms is one of most effective strategies to produce HRIPs. Taking advantage of

sulfur conversion through the present MCP, **P5** possessed a high refractive index of 1.725 to 1.701 from 600 to 1700 nm (Figure 2), in line with expectations. Furthermore, **P3** presents

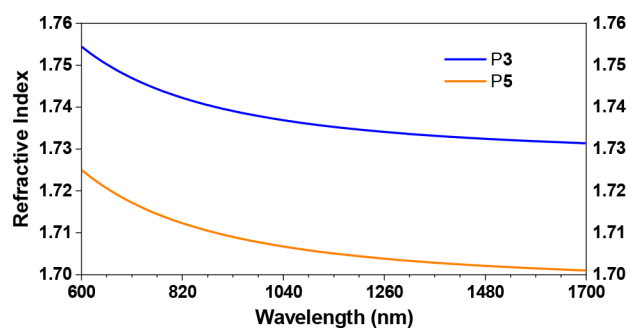


Figure 2. Light refraction spectra of thin solid films of poly(*O*-thiocarbamate)s.

higher n of 1.755 to 1.730 at the same wavelength window when more sulfur atoms were introduced accompanying diphenyl sulfide in **2c**. The poly(*O*-thiocarbamate)s prepared from this sulfur-based MCP are hence promising candidates for advanced optical materials.

Mercury Detection Application of Poly(*O*-thiocarbamate)s and Its Coordination Mode. Tetraphenylethylene (TPE) is a typical luminogen exhibiting an aggregation-induced emission (AIE) feature.⁵⁷ When TPE was introduced into polymers as an intentional design, **P4** and **P5** showed the expected AIE characteristics. As shown in Figures 3 and S13, the polymers did not fluoresce in the mixtures of tetrahydrofuran (THF)/water when the water fraction (f_w , by volume) was low. With the increase of f_w , aggregates of polymers formed due to the decreased solubility. A sharp enhancement of fluorescence under UV light was observed for the system when f_w was higher than a certain value. Taking **P4** as an example, there was an obvious

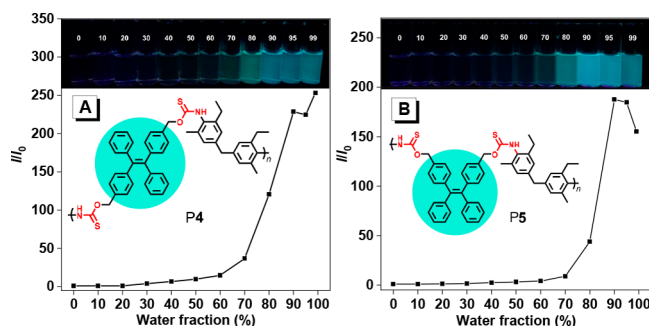


Figure 3. Plots of relative PL intensity versus water fractions (by volume) in THF/water mixtures of (A) P4 and (B) P5. Concentration of polymers: 10 μ M. Excitation wavelength: 360 nm.

aggregation/fluorescent turning point at 60% water content. This turning point could be used for turn-on detection based on AIE mechanism.

Poly(*O*-thiocarbamate)s are expected to show metal complexation because the thione groups have strong binding affinity to heavy metal ions.⁵⁷ If P4 dispersing in THF/H₂O ($f_w = 60\%$) did coordinate some metal ions, aggregation would occur to polymer segments because the metal cations played the role of cross-linking points by coordinating with adjacent thione group. Meanwhile, the coordination decreased the water solubility of the poly(*O*-thiocarbamate)s for the reduced free thione groups. As a result, the fluorescence of P4 would be turned on as it was excited under UV light.

To prove the above deduction, P4 was selected as an example to demonstrate the interaction between poly(*O*-thiocarbamate)s and different metal ions. The preliminary results are shown in Figures 4 and S14–S16. As revealed by the experimental data, the solution of P4 responded to both Hg²⁺ and Ag⁺ with positive signals (Figure 4A,B). However, when a screening agent of KBr was used, Hg²⁺ could be detected solely, and Ag⁺ was successfully shielded; meanwhile, other metal ions remained nonfluorescent, regardless of addition of the screening agent or not (Figure 4C,D). Using this method, the detection of Hg²⁺ in the presence of various metal ions was successful with AIE-active polymer P4 (Figure S14). Then the response speed was tested, and the fluorescence turn-on reached equilibrium after 10 min (Figure S15). The fluorescence intensity at 474 nm showed a great linear correlation with the concentrations of Hg²⁺ from 0 to 7.5 μ M. The limit of detection (LOD) was calculated to be 32 nM according to the equation of $LOD = 3SB/m$ (Figure S16).

Mercury is a global contaminant because it can travel a long distance through the atmosphere, resulting in wide distribution of Hg in water, air, and soil.^{58,59} Since knowledge of the toxicity of mercury was intensified following the deaths of hundreds of people caused by Minamata disease in Japan in the 1950s, the hazards of mercury have been highly addressed by scientists around the world.⁶⁰ To date, environmental mercury contamination is still a great threat to our world, and numerous studies have been made to detect mercury ions.^{33–46} As indicated by the experimental results, TPE-containing poly(*O*-thiocarbamate)s prepared from this MCP route can be used to detect mercury ion in a turn-on mode with high selectivity and sensitivity, which are promising for fluorescent chemosensors for Hg²⁺.

It is of great significance to address the coordination mode between thione groups and Hg²⁺ because of the importance of

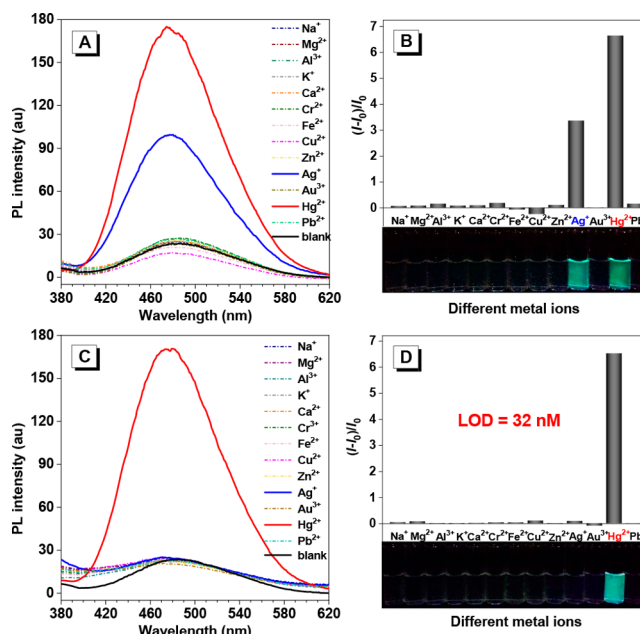


Figure 4. (A) PL spectra of P4 in THF/water mixtures (v/v: 4/6) with the presence of different metal ions (10 μ M). (B) Relative intensity ($I/I_0 - 1$) at 474 nm of P4 in THF/H₂O mixture (v/v: 4/6, 10 μ M) in the presence of different metal ions (10 μ M) and the corresponding fluorescence photos taken under UV irradiation. I_0 = PL intensity in the absence of metal ions. Excitation wavelength: 360 nm. (C, D) PL spectra and relative intensity of P4 when KBr (100 μ M) was added in each test mixture, other all conditions remain same with A and B respectively.

Hg²⁺ detection. However, the exact coordination between probes and heavy-metal ions has historically been vague. Some hypotheses were previously reported without explicit structures. To identify the coordination mode between P4 and mercury ion, tabular crystals of model compound M1 were dissolved and mixed with HgCl₂ in ethanol/water solution (Scheme S4), and acicular crystals were obtained eventually. With the X-ray single-crystal structural analyses, the coordination structure was veritably confirmed (Figure 5A, Table S3). Different from previous reports, two S atoms and two Cl atoms simultaneously participated in the coordination, while N atoms did not, affording an unforeseen tetracoordination structure. More subtly, well-defined features were revealed by the crystallographic data. The complex geometry was unsymmetrical; for example, the distances between Hg and two S atoms were 2.538 and 2.457 Å, respectively, and there were intra- and intermolecular interactions through Cl...H and Cl...S (Figure 5B). Hereto, the coordination mode between thione groups of P4 and mercury ion was clearly characterized (Figure 5C). This is an unprecedented insight of the interactions between Hg²⁺ and sulfur-containing functionalities. It may lead to important advances in dealing with environmental mercury contamination.

CONCLUSIONS

In this work, economic one-step conversion from elemental sulfur to functional poly(*O*-thiocarbamate)s through a transition-metal free multicomponent polymerization of sulfur, diols, and diisocyanides is realized. The detailed conditions for the polymerization reaction were systematically explored. The experimental results indicated that this MCP possesses unique

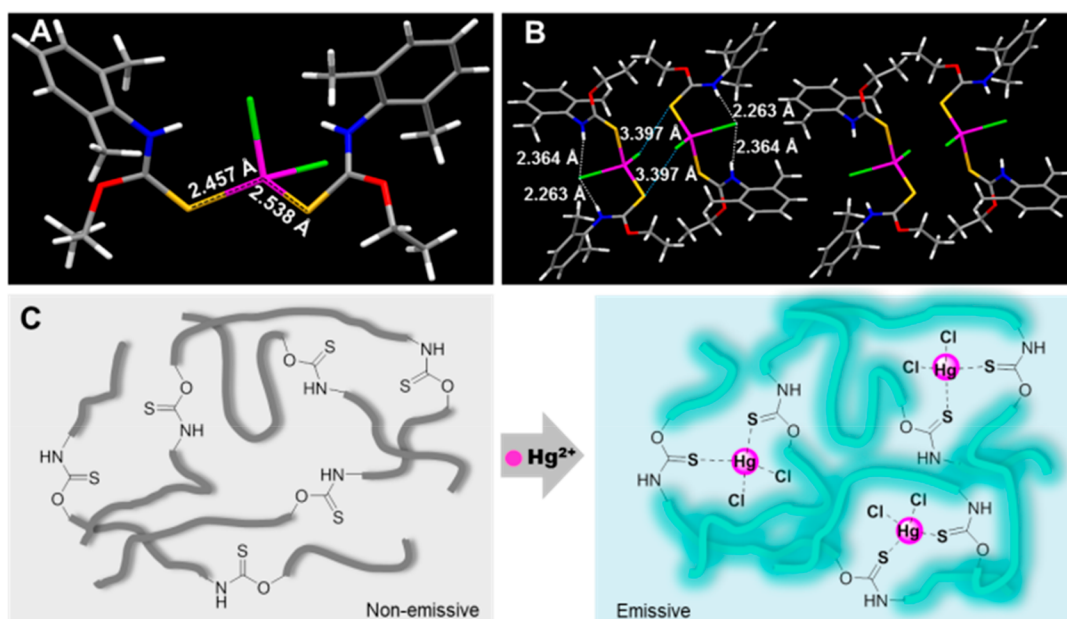


Figure 5. (A) X-ray single crystal structure of M2. (B) Crystal packing of M2. (C) Schematic diagram of detection on Hg^{2+} with P4.

advantages of mild conditions, short reaction time, high efficiency, high atom economy, and convenience, producing soluble poly(*O*-thiocarbamate)s with high yields, large M_w , and great diversity of well-defined polymer structures. Therefore, a novel MCP has been established. The present MCP route breaks the dependency on amide monomers, taking the generalization of sulfur conversion one step further. Meanwhile, the poly(*O*-thiocarbamate)s containing higher sulfur content show a high refractive index above 1.7 from 600 to 1700 nm and are ideal candidates as advanced optical materials. The poly(*O*-thiocarbamate)s can also be designed as turn-on type fluorescent chemo-sensors by introducing TPE moieties into the polymer skeleton. On the basis of the AIE-activity of TPE moieties, the selective, sensitive, and “turn-on” detection of mercury ion are successfully realized. More importantly, the coordination structures between poly(*O*-thiocarbamate)s and mercury ion are proven to be a tetracoordination mode using a single crystal of model coordination compound, which is first revealed here.

■ ASSOCIATED CONTENT

Supporting Information

The Supporting Information is available free of charge at <https://pubs.acs.org/doi/10.1021/jacs.1c00243>.

Materials, instruments, synthetic and experimental procedures, and characterization data; procedures for detection on mercury ion; optimization on the polymerization; the proposed reaction mechanism; thermogravimetric analysis of P1–P7; FT-IR spectra and ^1H and ^{13}C NMR spectra of 1c–1e, 2b, M1, M2, and P1–P7 (Figures S17–S28) (PDF)

Accession Codes

CCDC 2023847 and 2034126 contain the supplementary crystallographic data for this paper. These data can be obtained free of charge via www.ccdc.cam.ac.uk/data_request/cif, or by emailing data_request@ccdc.cam.ac.uk, or by contacting The Cambridge Crystallographic Data Centre, 12 Union Road, Cambridge CB2 1EZ, UK; fax: +44 1223 336033.

■ AUTHOR INFORMATION

Corresponding Authors

Jing Zhi Sun – MOE Key Laboratory of Macromolecules Synthesis of Functionalization, Department of Polymer Science and Engineering, Zhejiang University, Hangzhou 310027, China; orcid.org/0000-0001-5478-5841; Email: sunjz@zju.edu.cn

Ben Zhong Tang – MOE Key Laboratory of Macromolecules Synthesis of Functionalization, Department of Polymer Science and Engineering, Zhejiang University, Hangzhou 310027, China; Department of Chemistry, Hong Kong Branch of Chinese National Engineering Research Center for Tissue Restoration and Reconstruction, the Hong Kong University of Science & Technology, Kowloon, Hong Kong, China; orcid.org/0000-0002-0293-964X; Email: tangbenz@ust.hk

Authors

Jie Zhang – MOE Key Laboratory of Macromolecules Synthesis of Functionalization, Department of Polymer Science and Engineering, Zhejiang University, Hangzhou 310027, China; orcid.org/0000-0003-1641-1042

Qiguang Zang – MOE Key Laboratory of Macromolecules Synthesis of Functionalization, Department of Polymer Science and Engineering, Zhejiang University, Hangzhou 310027, China

Fulin Yang – MOE Key Laboratory of Macromolecules Synthesis of Functionalization, Department of Polymer Science and Engineering, Zhejiang University, Hangzhou 310027, China

Haoke Zhang – MOE Key Laboratory of Macromolecules Synthesis of Functionalization, Department of Polymer Science and Engineering, Zhejiang University, Hangzhou 310027, China; orcid.org/0000-0001-7309-2506

Complete contact information is available at: <https://pubs.acs.org/doi/10.1021/jacs.1c00243>

Author Contributions

Monomer and polymer synthesis, structure characterization, property investigation and manuscript preparation were performed by J.Z. Figure improvement, graphical abstract design, and fluorescent detection were performed by Q.Z. F.Y. helped with polymer synthesis and data analysis. Theoretical calculation and crystallographic data treatments were performed by H.Z. Guidance on research and manuscript writing, review, and editing was performed by J.Z.S. and B.Z.T.

Notes

The authors declare no competing financial interest.

ACKNOWLEDGMENTS

This work was financially supported by the National Science Foundation of China (22021715 and 51573158) and Zhejiang Province Department of Science & Technology (major scientific and technological project: 2020C03030).

REFERENCES

- (1) Greenwood, N. N.; Earnshaw, A. *Chemistry of the Elements*, 2nd ed.; Butterworth-Heinemann: Oxford, 1997.
- (2) Meyer, B. Elemental Sulfur. *Chem. Rev.* **1976**, *76*, 367–388.
- (3) Boulegue, J. Solubility of Elemental Sulfur in Water at 298 K. *Phosphorus Sulfur Relat. Elem.* **1978**, *5*, 127–128.
- (4) Steudel, R. Properties of Sulfur-Sulfur Bonds. *Angew. Chem., Int. Ed. Engl.* **1975**, *14*, 655–664.
- (5) Raines, R. T. Nature's Transitory Covalent Bond. *Nat. Struct. Biol.* **1997**, *4*, 425–427.
- (6) Rose, K.; Shadle, S. E.; Glaser, T.; deVries, S.; Cherepanov, A.; Canters, G. W.; Hedman, B.; Hodgson, K. O.; Solomon, E. I. Investigation of the Electronic Structure of 2Fe-2S Model Complexes and the Rieske Protein Using Ligand K-Edge X-ray Absorption Spectroscopy. *J. Am. Chem. Soc.* **1999**, *121*, 2353–2363.
- (7) Wu, X.; Smith, J. A.; Petcher, S.; Zhang, B.; Parker, D. J.; Griffin, J. M.; Hasell, T. Catalytic Inverse Vulcanization. *Nat. Commun.* **2019**, *10*, 647.
- (8) Boyd, D. A. Sulfur and Its Role In Modern Materials Science. *Angew. Chem., Int. Ed.* **2016**, *55*, 15486–15502.
- (9) Lovett, R. A. Rare Sulphur Dominates the Deep. *Science* **2011**, *331*, 1018–1019.
- (10) Pokrovski, G. S.; Dubrovinsky, L. The S₃⁻ Ion Is Stable in Geological Fluids at Elevated Temperatures and Pressures. *Science* **2011**, *331*, 1052–1054.
- (11) Pokrovski, G. S.; Kokh, M. A.; Guillaume, D.; Borisova, A. Y.; Gisquet, P.; Hazemann, J. L.; Lahera, E.; Del Net, W.; Proux, O.; Testemale, D.; Haigis, V.; Jonchière, R.; Seitsonen, A. P.; Ferlat, G.; Vuilleumier, R.; Saitta, A. M.; Boiron, M. C.; Dubessy, J. Sulfur Radical Species Form Gold Deposits On Earth. *Proc. Natl. Acad. Sci. U. S. A.* **2015**, *112*, 13484–13489.
- (12) Beinert, H. A Tribute to Sulfur. *Eur. J. Biochem.* **2000**, *267*, 5657–5664.
- (13) Nguyen, T. B.; Retailleau, P. Sulfur-Promoted DABCO Catalyzed Oxidative Trimerization of Phenylacetonitriles. *J. Org. Chem.* **2019**, *84*, 5907–5912.
- (14) Torres, M. E. S.; Morales, A. R.; Peralta, A. S.; Kroneck, P. M. H. Sulfur, The Versatile Non-Metal. *Met. Ions Life Sci.* **2020**, *20*, 19–49.
- (15) Chung, W. J.; Griebel, J. J.; Kim, E. T.; Yoon, H.; Simmonds, A. G.; Ji, H. J.; Dirlam, P. T.; Glass, R. S.; Wie, J. J.; Nguyen, N. A.; Guralnick, B. W.; Park, J.; Somogyi, Á.; Theato, P.; Mackay, M. E.; Sung, Y. E.; Char, K.; Pyun, J. The Use of Elemental Sulfur As An Alternative Feedstock for Polymeric Materials. *Nat. Chem.* **2013**, *5*, 518–524.
- (16) Kausar, A.; Zulfiqar, S.; Sarwar, M. I. Recent Developments in Sulfur-Containing Polymers. *Polym. Rev.* **2014**, *54*, 185–267.
- (17) Sun, Z.; Huang, H.; Li, L.; Liu, L.; Chen, Y. Polythioamides of High Refractive Index By Direct Polymerization of Aliphatic Primary Diamines in the Presence of Elemental Sulfur. *Macromolecules* **2017**, *50*, 8505–8511.
- (18) Fukuzaki, N.; Higashihara, T.; Ando, S.; Ueda, M. Synthesis and Characterization of Highly Refractive Polyimides Derived from Thiophene-Containing Aromatic Diamines and Aromatic Dianhydrides. *Macromolecules* **2010**, *43*, 1836–1843.
- (19) You, N. H.; Fukuzaki, N.; Suzuki, Y.; Nakamura, Y.; Higashihara, T.; Ando, S.; Ueda, M. Synthesis of High-Refractive Index Polyimide Containing Selenophene Unit. *J. Polym. Sci., Part A: Polym. Chem.* **2009**, *47*, 4428–4434.
- (20) Higashihara, T.; Ueda, M. Recent Progress in High Refractive Index Polymers. *Macromolecules* **2015**, *48*, 1915–1929.
- (21) Griebel, J. J.; Namnabat, S.; Kim, E. T.; Himmelhüber, R.; Moronta, D. H.; Chung, W. J.; Simmonds, A. G.; Kim, K. J.; Laan, J.; Nguyen, N. A.; Dereniak, E. L.; Mackay, M. E.; Char, K.; Glass, R. S.; Norwood, R. A.; Pyun, J. New Infrared Transmitting Material via Inverse Vulcanization of Elemental Sulfur to Prepare High Refractive Index Polymers. *Adv. Mater.* **2014**, *26*, 3014–3018.
- (22) Kawai, Y.; Kanbara, T.; Hasegawa, K. Preparation of Polythioamides from Dialdehydes and 4, 4'-Trimethylenedipiperidine with Sulfur by the Willgerodt-Kindler reaction. *J. Polym. Sci., Part A: Polym. Chem.* **1999**, *37*, 1737–1740.
- (23) Kanbara, T.; Kawai, Y.; Hasegawa, K.; Morita, H.; Yamamoto, T. Preparation of Polythioamides from Dialdehydes and Diamines with Sulfur by the Willgerodt-Kindler Type Reaction. *J. Polym. Sci., Part A: Polym. Chem.* **2001**, *39*, 3739–3750.
- (24) Li, W.; Wu, X.; Zhao, Z.; Qin, A.; Hu, R.; Tang, B. Z. Catalyst-Free, Atom-Economic, Multicomponent Polymerizations of Aromatic Dienes, Elemental Sulfur, and Aliphatic Diamines toward Luminescent Polythioamides. *Macromolecules* **2015**, *48*, 7747–7754.
- (25) Tian, T.; Hu, R.; Tang, B. Z. Room Temperature One-Step Conversion from Elemental Sulfur to Functional Polythioureas through Catalyst-Free Multicomponent Polymerizations. *J. Am. Chem. Soc.* **2018**, *140*, 6156–6163.
- (26) Cao, W.; Dai, F.; Hu, R.; Tang, B. Z. Economic Sulfur Conversion to Functional Polythioamides through Catalyst-Free Multicomponent Polymerizations of Sulfur, Acids, and Amines. *J. Am. Chem. Soc.* **2020**, *142*, 978–986.
- (27) Wręczycki, J.; Bielinski, D. M.; Kozanecki, M.; Maczugowska, P.; Mloston, G. Anionic Copolymerization of Styrene Sulfide with Elemental Sulfur (S₈). *Materials* **2020**, *13*, 2597.
- (28) Ding, Y.; Hay, A. S. Copolymerization of Elemental Sulfur with Cyclic (Arylene Disulfide) Oligomers. *J. Polym. Sci., Part A: Polym. Chem.* **1997**, *35*, 2961–2968.
- (29) Kuroda, H.; Tomita, I.; Endo, T. A Novel Polyaddition of Diols with Bifunctional Acetylenes Having Electron-Withdrawing Groups. *Macromolecules* **1995**, *28*, 433–436.
- (30) Imahori, T.; Hori, C.; Kondo, Y. Functionalization of Alkynes Catalyzed by t-Bu-P₄ Base. *Adv. Synth. Catal.* **2004**, *346*, 1090–1092.
- (31) Wang, J.; Li, B.; Xin, D.; Hu, R.; Zhao, Z.; Qin, Z.; Tang, B. Z. Superbase Catalyzed Regio-selective Polyhydroalkoxylation of Alkynes: a Facile Route towards Functional Poly(vinyl ether)s. *Polym. Chem.* **2017**, *8*, 2713–2722.
- (32) Németh, A. G.; Keserű, G. M.; Ábrányi-Balogh, P. A Novel Three-Component Reaction Between Isocyanides, Alcohols or Thiols and Elemental Sulfur: A Mild, Catalyst-Free Approach towards O-Thiocarbamates and Dithiocarbamates. *Beilstein J. Org. Chem.* **2019**, *15*, 1523–1533.
- (33) Hatai, J.; Pal, S.; Jose, G. P.; Bandyopadhyay, S. Histidine Based Fluorescence Sensor Detects Hg²⁺ in Solution, Paper Strips, and in Cells. *Inorg. Chem.* **2012**, *51*, 10129–10135.
- (34) Nolan, E. M.; Lippard, S. J. Tools and Tactics for the Optical Detection of Mercuric Ion. *Chem. Rev.* **2008**, *108*, 3443–3480.
- (35) Zhang, J. F.; Kim, J. S. Small-Molecule Fluorescent Chemosensors for Hg²⁺ Ion. *Anal. Sci.* **2009**, *25*, 1271–1281.
- (36) Valeur, B.; Leray, I. Design Principles of Fluorescent Molecular Sensors for Cation Recognition. *Coord. Chem. Rev.* **2000**, *205*, 3–40.

- (37) Prodi, L.; Bolletta, F.; Montalti, M.; Zaccheroni, N. Luminescent Chemosensors for Transition Metal Ions. *Coord. Chem. Rev.* **2000**, *205*, 59–83.
- (38) Métivier, R.; Leray, I.; Valeur, B. Lead and Mercury Sensing by Calixarene-Based Fluoroionophores Bearing Two or Four Dansyl Fluorophores. *Chem. - Eur. J.* **2004**, *10*, 4480–4490.
- (39) Chen, L.; Yang, L.; Li, H.; Gao, Y.; Deng, D.; Wu, Y.; Ma, L. Tridentate Lysine-Based Fluorescent Sensor for Hg(II) in Aqueous Solution. *Inorg. Chem.* **2011**, *50*, 10028–10032.
- (40) Ma, L.; Li, Y.; Li, L.; Sun, J.; Tian, C.; Wu, Y. A Protein-Supported Fluorescent Reagent for The Highly-Sensitive and Selective Detection of Mercury Ions in Aqueous Solution and Live Cells. *Chem. Commun.* **2008**, *47*, 6345–6347.
- (41) Li, H.; Li, Y.; Dang, Y.; Ma, L.; Wu, Y.; Hou, G.; Wu, L. An Easily Prepared Hypersensitive Water-Soluble Fluorescent Probe for Mercury(II) Ions. *Chem. Commun.* **2009**, *29*, 4453–4455.
- (42) Yang, M.; Thirupathi, P.; Lee, K. Selective and Sensitive Ratiometric Detection of Hg(II) Ions Using a Simple Amino Acid Based Sensor. *Org. Lett.* **2011**, *13*, 5028–5031.
- (43) Torrado, A.; Walkup, G. K.; Imperiali, B. Exploiting Polypeptide Motifs for the Design of Selective Cu(II) Ion Chemosensors. *J. Am. Chem. Soc.* **1998**, *120*, 609–610.
- (44) Aderinto, S. O. Fluorescent, Colourimetric, and Ratiometric Probes Based on Diverse Fluorophore Motifs for Mercuric(II) Ion (Hg²⁺) Sensing: Highlights from 2011 to 2019. *Chem. Pap.* **2020**, *74*, 3195–3232.
- (45) Duan, J.; Zhan, J. Recent Developments on Nanomaterials-Based Optical Sensors for Hg²⁺ Detection. *Sci. China Mater.* **2015**, *58*, 223–240.
- (46) Mahato, P.; Saha, S.; Das, P.; Agarwalla, H.; Das, A. An Overview of the Recent Developments on Hg²⁺ Recognition. *RSC Adv.* **2014**, *4*, 36140–36174.
- (47) Yanagisawa, Y.; Nan, Y.; Okuro, K.; Aida, T. Mechanically Robust, Readily Repairable Polymers via Tailored Noncovalent Cross-Linking. *Science* **2018**, *359*, 72–76.
- (48) Degani, I.; Fochi, R.; Magistris, C. O, S-Dimethyl Carbonodithioate as a Phosgene Substitute for the Preparation of S-Methyl Alkylcarbamothioates and Dialkylcarbamothioates. *Synthesis* **2009**, 3807–3818.
- (49) Reynaud, P.; Brion, J.; Davrinche, C.; Dao, P. O-Ethyl Thiocarbamates. A Convenient Route to 2-Aryliminoimidazolidines. *J. Heterocycl. Chem.* **1980**, *17*, 1789–1792.
- (50) Ma, H.; Jen, A. K. Y.; Dalton, L. R. Polymer-Based Optical Waveguides: Materials, Processing, and Devices. *Adv. Mater.* **2002**, *14*, 1339–1365.
- (51) An, N.; Wang, K.; Wei, H.; Song, Q.; Xiao, S. Fabricating High Refractive Index Titanium Dioxide Film Using Electron Beam Evaporation for All-Dielectric Metasurfaces. *MRS Commun.* **2016**, *6*, 77–83.
- (52) Brandrup, J.; Immergut, E. H.; Grulke, E. A. *Polymer Handbook*, 4th ed.; Wiley: New York, 2004.
- (53) Mark, J. E. *Polymer Data Handbook*, 2nd ed.; Oxford Univ. Press: New York, 2009.
- (54) Kim, D. W.; Han, J. W.; Lim, K. T.; Kim, Y. H. Highly Enhanced Light-Outcoupling Efficiency in ITO-Free Organic Light-Emitting Diodes Using Surface Nanostructure Embedded High-Refractive Index Polymers. *ACS Appl. Mater. Interfaces* **2018**, *10*, 985–991.
- (55) Liu, J.; Ueda, M. High Refractive Index Polymers: Fundamental Research and Practical Applications. *J. Mater. Chem.* **2009**, *19*, 8907–8919.
- (56) Ho, P. K. H. D.; Thomas, S.; Friend, R. H.; Tessler, N. All-Polymer Optoelectronic Devices. *Science* **1999**, *285*, 233–236.
- (57) Mei, J.; Leung, N. L. C.; Kwok, R. T. K.; Lam, J. W. Y.; Tang, B. Z. Aggregation-Induced Emission: Together We Shine, United We Soar! *Chem. Rev.* **2015**, *115*, 11718–11940.
- (58) Tang, Z.; Fan, F.; Deng, S.; Wang, D. Mercury in Rice Paddy Fields and How Does Some Agricultural Activities Affect the Translocation and Transformation of Mercury-A Critical Review. *Ecotoxicol. Environ. Saf.* **2020**, *202*, 110950.
- (59) Fitzgerald, W. F.; Lamborg, C. H.; Hammerschmidt, C. R. Marine Biogeochemical Cycling of Mercury. *Chem. Rev.* **2007**, *107*, 641–662.
- (60) Harada, M. Minamata Disease: Methylmercury Poisoning in Japan Caused by Environmental Pollution. *Crit. Rev. Toxicol.* **1995**, *25*, 1–24.